Drying Technology: An International Journal
Publication details, including instructions for authors and subscription information:
http://www.tandfonline.com/loi/ldrt20

Modeling of Microwave Drying of Fruits. Part II: Effect of Osmotic Pretreatment on the Microwave Dehydration Process

J. R. Arballo [a b], L. A. Campañone [a b] & R. H. Mascheroni [a b]

[a] Centro de Investigación y Desarrollo en Criotecnología de Alimentos (CIDCA), CCT La Plata, CONICET, UNLP, La Plata, Argentina

[b] MODIAL-Facultad Ingeniería, Universidad Nacional de La Plata, Argentina

Available online: 30 Jan 2012

To cite this article: J. R. Arballo, L. A. Campañone & R. H. Mascheroni (2012): Modeling of Microwave Drying of Fruits. Part II: Effect of Osmotic Pretreatment on the Microwave Dehydration Process, Drying Technology: An International Journal, 30:4, 404-415

To link to this article: http://dx.doi.org/10.1080/07373937.2011.645100

Drying Technology, 30: 404–415, 2012

ISSN: 0737-3937 print/1532-2300 online
DOI: 10.1080/07373937.2011.645100

Taylor & Francis
Taylor & Francis Group

Modeling of Microwave Drying of Fruits. Part II: Effect of Osmotic Pretreatment on the Microwave Dehydration Process

J. R. Arballo,[1,2] L. A. Campañone,[1,2] and R. H. Mascheroni[1,2]
[1]*Centro de Investigación y Desarrollo en Criotecnología de Alimentos (CIDCA), CCT La Plata, CONICET, UNLP, La Plata, Argentina*
[2]*MODIAL-Facultad Ingeniería, Universidad Nacional de La Plata, Argentina*

The heat and mass transfer during the combined process of osmotic–microwave drying (OD-MWD) of fruits was studied theoretically and experimentally through modeling and numerical simulation. With the aim of describing the transport phenomena involved in the combined dehydration process, the mass and energy microscopic balances were set out. For the first step (OD), two models with different levels of complexity were proposed, an osmotic–diffusive and a countercurrent flow diffusive model. For MWD, the energy and mass balances were solved, using moisture- and temperature-dependent properties; inner heat generation due to transformation of the electromagnetic energy was accounted for by using the approximation of Lambert's law. The numerical solution obtained from OD was incorporated as initial values for the simulation of MWD. The model validation was satisfactorily carried out in pears, both fresh and osmodehydrated for 2 h in sucrose solutions and then irradiated in a microwave oven at 500 W. From the results it was observed that a higher dehydration rate was reached during microwave drying when the fruits were pretreated with 40 and 60°Brix sucrose solution.

Keywords Fruits; Mathematical modeling; Osmotic–microwave drying

INTRODUCTION

Osmotic dehydration (OD) has the ability to protect food for further drying treatments, decreasing the losses in volatile compounds and the risk of chemical and physical changes. It involves immersion in a hypertonic solution that results in partial water removal. To complete the drying process and obtain a stable product, a further procedure such as microwave drying (MWD) is necessary. Microwaves have the ability to penetrate and generate volumetric heat within the product, due to the interaction of the electric field with water molecules, increasing the vapor pressure and therefore the driving force of the dehydration process.[1] When using microwaves as a final drying stage, several advantages exist compared to traditional drying processes: lower environmental impact due to the use of clean energy and low energy consumption in addition to reduced space and processing time requirements.

The transport phenomena during the combined dehydration process include several mass transfer mechanisms. During OD, the simultaneous mass transfer of water and solids between the food and the osmotic solution has to be considered. From a microscopic point of view, the mass transfer involves the water flux through cellular membranes and multicomponent diffusion across intercellular spaces. During MWD, complex mass transfer mechanisms take place (diffusion of water, liquid, and vapor; capillary flow; Knudsen diffusion; hydrodynamic flow). The product composition at the end of the OD process (moisture and soluble solids content and profile) determines the radiation–food interaction capacity through the variation in dielectric properties. These properties are responsible for MW heating and dehydration due to the interaction of the electric field with the polar molecules. Several authors have demonstrated the change in dielectric properties of products with different water and sugar contents.[2–5] In addition several research works have reported the dependence of the dielectric properties of sugar solutions on their composition.[6,7]

With respect to modeling of these processes, there exist models to simulate the mass transfer phenomena during osmotic dehydration that cover a wide range of physical approaches and mathematical descriptions. They can be divided into two groups: phenomenological and microscopic–structural. The first relate the water loss, solids gain, and weight reduction with operating conditions by simple empirical equations, whose validity is limited to the case under study.[8,9] The most simplified microscopic–structural models consider diffusion in a homogeneous system and solve the microscopic mass balance employing the

Correspondence: J. R. Arballo, Centro de Investigación y Desarrollo en Criotecnología de Alimentos, CCT La Plata, CONICET, UNLP, Calle 47 y 116, La Plata 1900, Argentina; E-mail: jrarballo@cidca.org.ar

analytical solution of Fick's second law. Then apparent diffusion coefficients are calculated for each component by fitting experimental data.[10] In the same group, there are highly elaborated models such as those developed by Marcotte and Le Maguer[11] and Yao and Le Maguer.[12] These models combine multicomponent diffusion with the existence of structural elements (e.g., cellular wall, protoplasmatic membrane, intercellular spaces) that add greater resistance and generate the appearance of numerous coefficients, which are difficult to calculate and measure.[13] With the purpose of simplifying the modeling of osmotic dehydration, some authors have numerically solved the diffusion equation considering a constant diffusion coefficient or took into account volume reduction during the process,[14] which allows the model to predict moisture and soluble solids profiles with adequate accuracy.

Several authors have modeled microwave dehydration.[15,16] In the present work, the study was focused on the energy and mass transfer due to the interaction between microwaves and food. This interaction is affected by the change in the food's properties due to the incorporation of osmotic medium and moisture loss during the pretreatment (OD). Lambert's law was used to model this interaction to obtain electromagnetic field distribution inside the samples. This law is incorporated into the energy balance as a source term to obtain temperature profiles for different microwave heating conditions. This simplified law has been successfully used in several previous works dealing with heating and dehydration.[17–20] With respect to mass transfer, it must be considered that dehydration occurs in two principal stages, an initial stage of weak evaporation and another of intense evaporation, which have to be modeled independently.[20]

Many researchers have experimentally studied the combined OD-MWD process. Venkatachalapathy and Raghavan[21] studied the OD-MWD of strawberries to analyze the effect of velocity and process time on the quality parameters of dried fruits. Beaudry et al.[22,23] studied the drying of cranberries that had been previously partially dehydrated by osmosis in a high-fructose corn syrup employing OD combined with microwaves and hot air. Fumagalli and Silveira[24] examined the effect of OD operating conditions and microwave power on the quality of dried pears. Andrés et al.[25] presented an experimental work on OD-MWD of mango, and Corrêa et al.[26] applied microwave–vacuum (MW-V) with osmotic dehydration (OD) as a pretreatment to pineapples.

However, none of these studies related the sugar uptake during the OD process with the change in dielectric properties. These properties govern the radiation–food interaction, especially during the last drying stage (MWD), dramatically affecting the dehydration kinetics.

The goal of this work is to develop a numerical model of the combined OD-MWD process in order to accurately determine the water loss and solids gain as final values during osmotic pretreatment and their influence on MWD treatment. To date this has not yet been investigated. In addition, processing times can be determined, which is useful information for food processors to correctly design equipment for combined processes and optimize the industrial production of dried fruits and vegetables.

According to the previous considerations the objectives of this work were as follows:

- To obtain an adequate numerical model that predicts process variables during osmotic dehydration followed by microwave application (OD-MWD) in order to solve the microscopic mass and energy balances.
- To solve the nonlinear mathematical model considering that the thermal, electromagnetic, and transport properties are temperature and composition dependent.
- To take into account the change in dielectric properties due to OD treatment to validate model predictions against experimental temperature and moisture data of OD-MWD pears.

MATERIALS AND METHODS

Mathematical Modeling

In the development of the mathematical model, two fundamental steps were considered: the OD process and the application of microwaves as a final drying step. A scheme of the osmotic–microwave dehydration model (1D slab) is shown in Figs. 1a and 1b.

Osmotic Dehydration Model

Two models, with different levels of complexity, were applied to predict the moisture and soluble solids content. Firstly, a previous model developed by Spiazzi and Mascheroni[13] was used and, secondly, a simpler countercurrent flow diffusive model was adopted.

Both models were proposed with the aim to evaluate the goodness of the prediction in the final OD values, which will be used later in microwave drying.

Osmotic–Diffusional Cellular Model (ODmodel-1). To model the osmotic dehydration process, the Spiazzi and Mascheroni[13] cellular model was used. The model formulation considers mass transfer through cellular membranes and multicomponent diffusion across intercellular spaces (Fig. 2). The volume representing the food material is divided into N concentric and equal volume elements. In each volume, two phases can be distinguished: the plasmatic content and the intercellular space. Each volume of intercellular space is subject to a diffusive–convective flux between adjacent volumes and a transmembrane diffusive

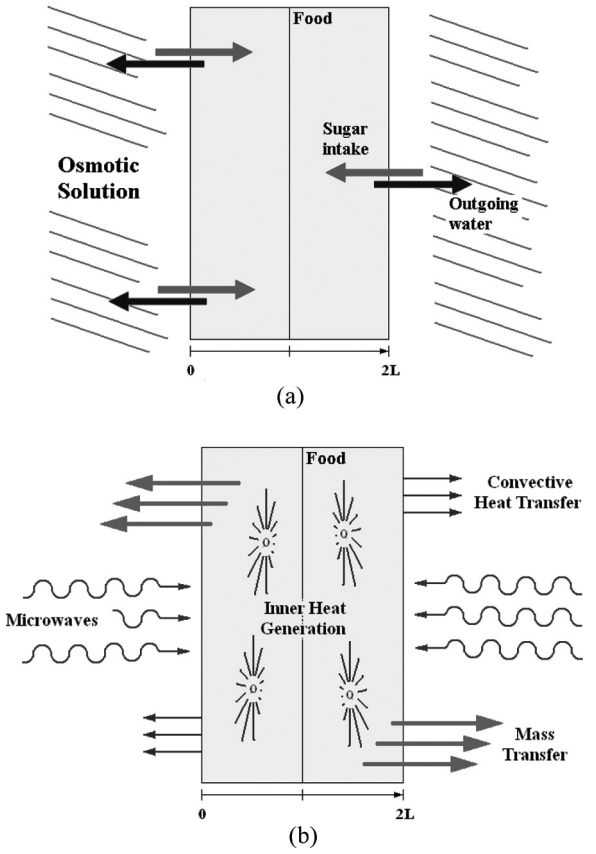

FIG. 1. (a) Scheme of the product slab and simultaneous mass fluxes taken into account by the countercurrent flow diffusive model; (b) Scheme of the product slab and mass and energy fluxes taken into account by the microwave drying model.

flux from the cell plasma. In this way, it is possible to transform the 2D problem into a 1D one and the grid is set up in a dimension normal to the surface.

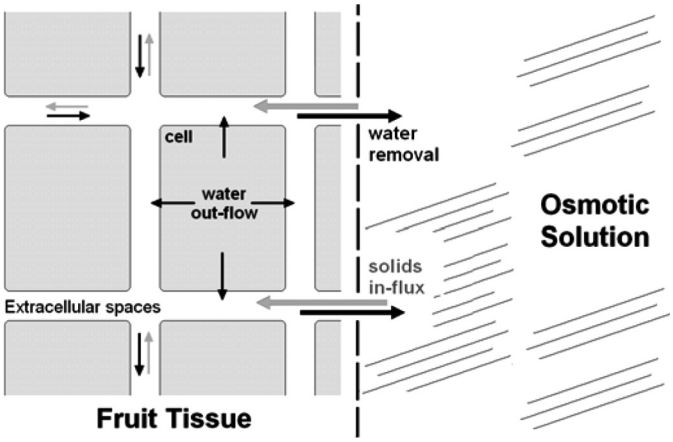

FIG. 2. Mass transfer mechanisms considered in the mass balance of the osmotic–diffusional cellular model.

The mass balances for water or sucrose ($j = w$ or s) in the cellular and extracellular volume i can be written as:

$$\frac{d(M_{j\text{int}})}{dt} = -(k_{w\text{int}}\Delta c_{j\text{int}})A_{\text{int}} \tag{1}$$

$$\frac{d(M_{j\text{ext}})}{dt} = \Delta[(D_{\text{app}j}\cdot\nabla(c_{j\text{ext}}) + c_{j\text{ext}}u)A_{\text{ext}}] + (k_{w\text{int}}\Delta c_{j\text{int}})A_{\text{int}} \tag{2}$$

where $M_{j\text{int}}$ and $M_{j\text{ext}}$ are the cellular and extracellular masses of component j correspondent to volume V_i, respectively; c_j is the concentration of component j; $k_{w\text{int}}$ is the transmembrane mass transfer coefficient; $D_{\text{app}j}$ corresponds to the apparent diffusion coefficient of component j in the extracellular space; A_{int} and A_{ext} are the transfer areas of cellular and extracellular volume, respectively; u is the shrinking rate; and t is the time.

The cellular and extracellular transfer areas can be calculated as follows:

$$A_{\text{int}} = N_{cell}V_{\text{int}}^{i\,2/3} \tag{3}$$

$$A_{\text{ext}} = C_g V_{\text{ext}}^{i\,2/3}\ell^i \tag{4}$$

where N_{cell} and C_g are constants that depend on the cell shape, the number of cells per unit volume, and shape of the product piece; V_{int} and V_{ext} are the cellular and extracellular volume; and ℓ^i represents the fraction of the geometric area that belongs to the extracellular spaces.

The apparent diffusion coefficient is defined as:

$$D_{\text{app}j} = \frac{D_{\text{ini}\,j}}{\mu^i} \tag{5}$$

where $D_{\text{ini}j}$ is the fitting coefficient for the model predictions and μ is the viscosity of the mixture that can be calculated as function of composition and concentration of the osmotic solution:[27]

$$\mu = \sum_j \frac{x_j}{(1-\phi)}\mu_j^0 \tag{6}$$

where x_j is the weight fraction of the species j, ϕ is the water content, and μ_j^0 is the viscosity of the solution of the species j with a water content equal to that of the mixture. The viscosity of some sugar solutions as a function of water concentration is presented as follows:

$$\mu_j^0 = \exp(aW^2 + bW + c) \tag{7}$$

where W is the water concentration (kg m^{-3}) and a, b, and c are parameters of the correlation.

Countercurrent Flow Diffusional Model (ODmodel-2) To obtain the moisture concentration profiles, the food was assumed as a homogeneous system and the osmotic dehydration was numerically modeled. The two countercurrent flows that take place during the osmotic process must be considered. Those simultaneous flows consist of an outgoing water flux from the food to the external solution and an inward solute flow from the osmotic solution to the vegetal tissue. In order to model the osmotic dehydration process, the following were assumed:

- One-dimensional mass transfer, infinite slabs (1D)
- Uniform initial water and soluble solids content in the whole product
- Concentration-dependent diffusion coefficient
- Isothermal process
- Surface concentration of sugar and water in the fruit are considered at equilibrium with osmotic solution concentration
- Shrinkage is neglected

To describe mass transfer, a mass balance must be developed for water and soluble solids. In order to describe the moisture and soluble solids transfer, Fick's second law was used:

$$\frac{\partial C_w}{\partial t} = \nabla(D_{w-s}\nabla C_w) \tag{8}$$

$$\frac{\partial C_s}{\partial t} = \nabla(D_{w-s}\nabla C_s) \tag{9}$$

where C_w and C_s are the concentration of water and soluble solids, respectively; t represents the time; and $D_{w\text{-}s}$ is the binary diffusion coefficient ($m^2\,s^{-1}$), which depends on outgoing water and incoming sugar.

Initial and boundary conditions also have to be considered to complete the model formulation:

$$t = 0 \qquad C_w = C_{w,ini}; \quad C_s = C_{s,ini} \qquad 0 \le x \le 2L \tag{10}$$

$$x = 0,\ 2L \qquad C_w = C_{w,eq}; \quad C_s = C_{s,eq} \qquad t > 0 \tag{11}$$

where $C_{w,eq}$ and $C_{s,eq}$ are the equilibrium concentration of water and soluble solids, respectively, and 0 and $2L$ correspond to both boundary sides of the slab.

The binary diffusion coefficient ($D_{w\text{-}s}$) can be calculated as a simultaneous function of the concentration of water and solids using the Stokes-Einstein equation:[28]

$$D_{w-s} = \frac{k_B\,T_{OD}}{6\,\pi\,r_B\,\mu_m} \tag{12}$$

where μ_m corresponds to the viscosity of the binary solution, k_B is the Boltzmann's constant, r_B is the solute apparent hydrodynamic radius, and T_{OD} is the product temperature during osmotic dehydration (K). The coefficient $D_{w\text{-}s}$ is a function of concentration values through the viscosity (μ_m) and can be calculated using Eq. (13):

$$\mu_m = \frac{(995 + 0.1284\ c'_s)^*\mu_w}{\rho_w}\left(1 + 0.73\frac{c'_s}{995 + 0.1284c'_s}\exp\left(\frac{\left(\frac{c'_s}{995+0.1284c'_s}\right)^{1.1}}{8.345\,(T_{OD}/273.16) - 7.402}\right)\right) \tag{13}$$

where μ_w is the viscosity of water (Pa s), ρ_w is the density of water ($kg\,m^{-3}$), and c'_s corresponds to the molar concentration of soluble solids ($mol\,m^{-3}$).

In addition, the concentration of water and soluble solids at equilibrium were obtained from experimental runs up to 24 h of osmotic dehydration.

Microwave Drying Model

In the final drying step, two stages must be considered: stage 1, heating with weak evaporation, and stage 2, intensive evaporation. In addition, the following assumptions were made when developing the microwave mathematical model:[20]

- Uniform initial temperature and water content within the product
- Temperature- and moisture content–dependent dielectric properties
- Volume changes are not considered
- Convective boundary conditions
- Regular one-dimensional geometry (1D)
- Uniform electric field distribution around the sample and a dominant polarization of the electric field normal to the surface

Heating with Weak Evaporation. Stage 1 involves the heating of the food up to the moment when the whole product reaches the equilibrium temperature T_{eq}. To describe heat transfer, an energy balance must be developed that considers a term of internal heat generation due to the energy supplied by MW.[29] The resulting microscopic energy balance in terms of power is

$$V\rho C_p\frac{\partial T}{\partial t} = V(\nabla k\nabla T) + P \tag{14}$$

where V is product volume (m^3), ρ is density ($kg\,m^{-3}$), C_p is the specific heat capacity ($J\,kg^{-1}{}^{\circ}C^{-1}$), T is temperature (°C), t is time (s), k is thermal conductivity ($W\,m^{-1}{}^{\circ}C^{-1}$), and P is the power generated by the absorption of

microwaves (W). In this balance, physical properties correspond to the fresh food.

To complete the model, the following initial and boundary conditions are considered:

$$t = 0 \qquad T = T_{\text{ini}} \qquad 0 \le x \le 2L \tag{15}$$

$$x = 0,\ 2L \quad -k\frac{\partial T}{\partial x} = h(T - T_a) + L_{\text{vap}}\, k_m(C_w - C_{eq}) \qquad t > 0 \tag{16}$$

The boundary condition (Eq. (16)) was used by several authors to model the initial heating step of the microwave drying process.[15,30] A value of 5 ($\text{W m}^{-2\circ}\text{C}^{-1}$) was employed for natural convection around the product slab (h). To evaluate the mass transfer coefficient k_m, the model considers the analogy between heat and mass transfer.[31]

The power absorbed during microwave irradiation on both sides (Fig. 3) is represented by the term P. Heat generation is a function of the temperature at each point of the material. In this work, Lambert's law is deemed as valid.[29]

$$P = P'_o(e^{-2\alpha(2L-x)} + e^{-2\alpha(x)}) \tag{17}$$

$$\alpha = \frac{2\pi}{\lambda}\sqrt{\frac{\varepsilon'\left[(1+\tan^2\delta)^{1/2} - 1\right]}{2}} \tag{18}$$

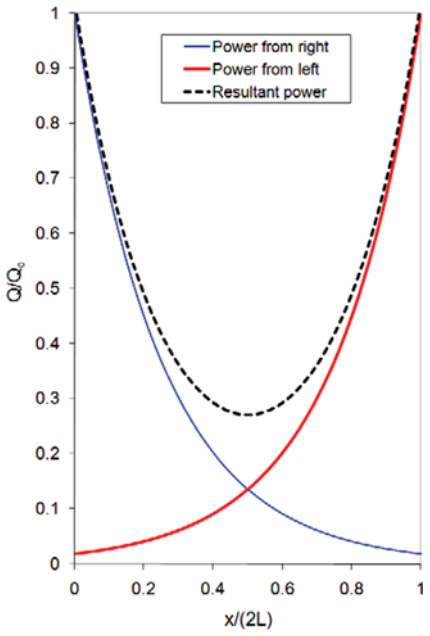

FIG. 3. Power absorbed in the whole food and power contributions from the microwaves on both sides of the material (color figure available online).

$$\delta = \tan^{-1}(\varepsilon''/\varepsilon') \tag{19}$$

where P'_o is the incident power at the surface (W), λ is the wavelength of radiation, and α is the attenuation factor, which is a function of the dielectric constant ε' and of the loss factor ε''.

To predict the humidity profile during the heating stage, a microscopic mass balance is required that considers the water diffusion in the inner part of the food. This balance is

$$\frac{\partial C_w}{\partial t} = \nabla(D_w \nabla C_w) \tag{20}$$

The following initial and boundary conditions are considered:

$$t = 0 \quad C_w = C_{w,\text{ini}} \quad 0 \le x \le 2L \tag{21}$$

$$x = 0,\ 2L \quad -D_w\frac{\partial C_w}{\partial x} = k_m(C_w - C_{eq}) \quad t > 0 \tag{22}$$

Intensive Evaporation. Stage 2 of microwave drying takes place when the whole product reaches T_{eq} and intensive evaporation begins. T_{eq} is the temperature achieved when the power absorbed is equilibrated with the energy used in water vaporization.[20] This step finishes at the end of the constant temperature period, unless there is a requirement to heat the material after it is dried. In the energy transfer step, the temperature is supposed to be at the equilibrium value in the whole food, T_{eq}

$$0 \le x \le 2L \quad T = T_{\text{eq}} \tag{23}$$

Lambert's law was applied to evaluate the distribution of electromagnetic energy inside the food. The following equation was applied:

$$P = P'_o(e^{-2\alpha_d(2L-x)} + e^{-2\alpha_d(x)}) \tag{24}$$

where α_d is the attenuation factor calculated using the dielectric properties of the dehydrated material, which are dependent on the osmotic pretreatment employed.

The model takes into account the continuous or intermittent application of MW power considering the incident microwave power to be zero when the magnetron is turned off in the cycling operation mode.

During this final stage, water vaporization is considered to take place volumetrically within the product. The generation of water vapor is calculated supposing that all of the power generated by MW is used for removal of water:[20]

$$m_v\, L_{\text{vap}} = \int_0^V Q\, dV \tag{25}$$

where m_v is the rate of water vaporization (kg s^{-1}).

Dehydration Experiments

Osmotic Dehydration

With the aim of validating the mathematical model, 15-mm-thick pear (var. Packham's Triumph) discs with a 55-mm diameter were used. The samples were weighed and introduced into beakers containing the hypertonic solution at different sucrose concentrations (20, 40, and 60°Brix), which were put into a thermostated shaker (model TT400, FERCA, Buenos Aires, Argentina) at constant shaking of 100 cycles/min. The employed solution–sample mass ratio was 10:1 to assure a constant concentration of the osmotic solution throughout the process. The first step of drying, osmotic dehydration, was carried out at a constant temperature of 30°C. After 2 h of dehydration, the samples were drained, placed on absorbent paper in order to remove the excess solution, and set on plastic trays to determine total final weight and water and soluble solids content. The experiments were done in triplicate.

Microwave Drying

Samples of fresh or osmodehydrated pear were placed in the MW oven in a single layer on a plastic mesh support, which is transparent to MW radiation and allows energy and mass transfer through both faces of the samples. The average mass of slices was 38.53 g (1.96 g SD) and the absorbed MW power density was in the order of $9\,Wg^{-1}$, considering that one sample was run in each individual experiment. The temperature of the fruit pieces was sensed online with accuracy of ± 1°C using a fiber optic sensor (model FOT-L-SD, Fiso Technologies Inc., Quebec, Canada) embedded in the geometric center of the sample.

Analytical Determinations

Microwave Power. The incident MW power (P_o) was determined using a calorimetric method. Distilled water was placed into Pyrex containers that had the same dimensions and were located in the same position in the MW oven as those of the samples during the drying experiments. The MW power calibration was performed with water volumes from 25 to 125 mL. Absorbed power was calculated calorimetrically using the following expression based on the increase in water temperature:[15]

$$P_o = m_w Cp_w \frac{\Delta T}{\Delta t} \tag{26}$$

where m_w is the mass of liquid water (kg), Cp_w is the specific heat of water, ΔT is the increment of temperature, and Δt is the heating time.

A polynomial model was proposed to relate power P_o (W) with the water content of the sample. Systat 10 Statistical software (Systat, Inc., Evanston, IL) was used to estimate the model parameters and to calculate their deviation. Figure 4 shows the experimental and calculated relationship between absorbed microwave power and the corresponding sample volume. The following empirical relations were obtained:

$$P_o = -0.0436V^2 + 11.855V \qquad V < 100\text{mL} \qquad R^2 = 0.976 \tag{27}$$

$$P_o = 700 \qquad V \geq 100\text{mL} \tag{28}$$

The values of P_o obtained with Eqs. (27) and (28) were then used as an input data in the solution of the microwave model.

To avoid thermal degradation (scorching), the samples were irradiated with a cycled power of 50% (10 s on and 10 s off with the oven switch set at 1,000 W). In addition to lowering the incident MW power, this mode of operation made it possible to control the overpressure generated inside the foods and prevent puffing and volume changes. To establish the drying kinetics, five independent runs with 1, 2, 3, 4, and 5 min of MW drying were performed under the same conditions.

Moisture

Moisture content of the samples was determined for the raw sample, the OD sample before drying, and the dry sample after each run by dehydration in a vacuum oven at 70°C and 65 kPa until a constant mass was attained.[32]

Soluble Solids

The soluble solids content of the fruit was determined by °Brix measurement at 20°C in a refractometer (Bellingham-Stanley Limited, Kent, UK).

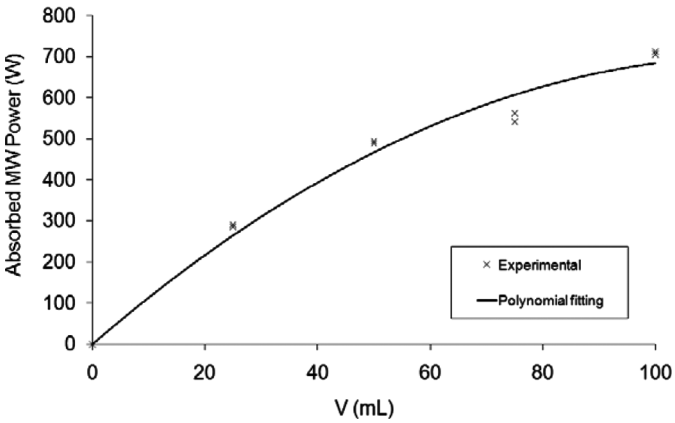

FIG. 4. Absorbed microwave power as a function of food water content expressed as sample water volume.

RESULTS AND DISCUSSION

Numerical Solution of the Combined Drying Process

The mass and energy balances obtained for the combined process of osmotic–microwave drying constitute a system of highly coupled nonlinear differential equations that were solved by applying numerical methods. For the osmotic–diffusional model (ODmodel-1) the mass balances for water and soluble solids constituted ordinary coupled differential equations that were solved using the fourth-order Runge-Kutta method with uniform initial moisture and soluble solids content in the whole product. With respect to the countercurrent flow diffusional model (ODmodel-2) the mass balances and their initial and boundary conditions for water and soluble solids form a system of nonlinear partial differential equations that were solved through an implicit scheme of finite differences. In the microwave heating stage the mass and energy balance are coupled. These balances, together with their boundary conditions, form a system of nonlinear partial differential equations that were solved using the Crank-Nicolson finite difference time-dependent method (FDTD), which is characterized as unconditionally stable and convergent. Then, the intensive evaporation stage was solved considering constant temperature (T_{eq}) in the whole sample and the electromagnetic energy distribution was calculated using Lambert's law with moisture-dependent electromagnetic properties; the outward vapor transport was calculated using Eq. (25).

Moisture and soluble solids content calculated for the final point of OD simulation were incorporated as initial values for the simulation of MWD. Time steps of 0.1 and 200 s were used for ODmodel-1 and ODmodel-2, respectively, and the domain was divided into 10 and 15 space increments for each osmotic model, respectively. In the case of the MWD model (second step), 25 space increments were used to divide the domain and a time increment of 0.1 s was used. A complete scheme of the solution algorithm using ODmodel-2 and the MWD model is shown in Fig. 5. The numerical methods were coded in MATLAB 7.2 (Mathworks, Natick, MA).

Model Validation

The complete OD-MWD model was validated against experimental data for temperature and moisture content obtained in our laboratory. The physical properties of fresh and osmodehydrated pears used in the mathematical modeling are summarized in Tables 1 and 2.

Figure 6a shows the numerical prediction for ODmodel-1 and ODmodel-2 and experimental data for osmodehydrated pears processed with three different solution concentrations (20, 40, and 60°Brix). As expected from the experimental results, it can be observed that increasing the concentration of hypertonic solution resulted in greater water removal.[33]

Moreover, the numerical predictions for both osmotic models obtained accurate moisture values at 2 h of the process (average relative error <0.25 and <0.12 for ODmodel-1 and -2, respectively). ODmodel-1 was previously validated for long processing times by other

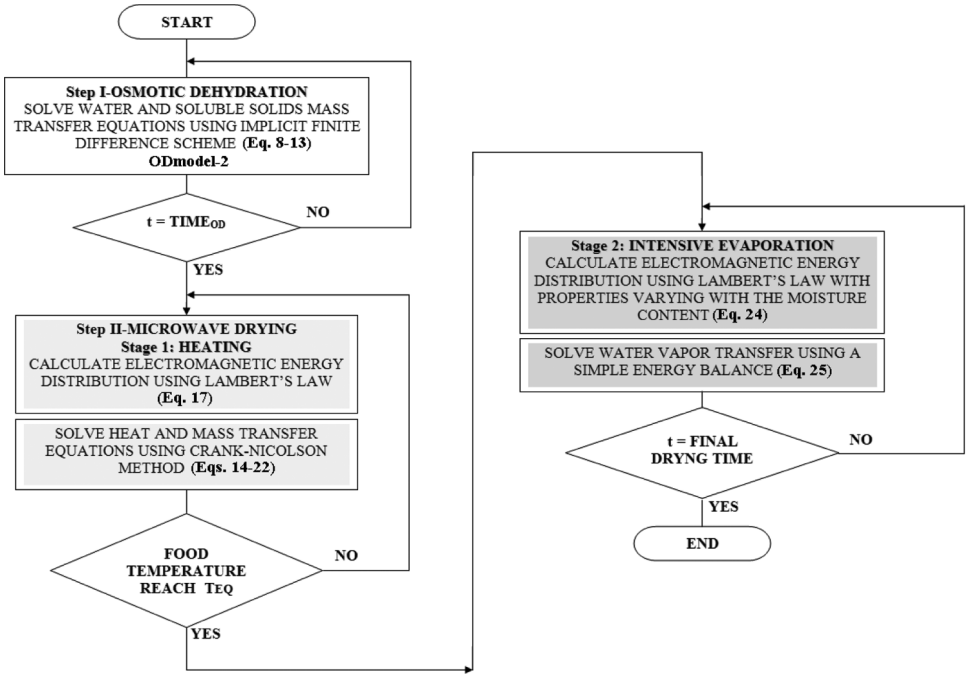

FIG. 5. Complete block diagram of solution algorithm for the osmotic–microwave drying model.

TABLE 1
Parameters and properties for osmotic dehydration models

Variable	Water	Soluble solids
	ODmodel-1	
kw_{int} ($m\,s^{-1}$)	200×10^{-9}	—
D_{iniw} ($m^2\,s^{-1}$)	1.36×10^{-9}	—
D_{inis}($m^2\,s^{-1}$)	—	0.17×10^{-9} (sucrose)
N_{cell} (cell constant)	1.275×10^{6}	—
C_g (shape constant)	2	—
a	—	13.116×10^{-6} (sucrose)
b	—	-28.47×10^{-3} (sucrose)
c	—	15.354 (sucrose)
	ODmodel-2	
C_{ini} ($kg\,kg^{-1}$ sample, wb)	0.856	0.115
C_{eq} ($kg\,kg^{-1}$ sample, wb)	0.8003 (20°Brix)	0.153 (20°Brix)
	0.6945 (40°Brix)	0.284 (40°Brix)
	0.5657 (60°Brix)	0.410 (60°Brix)
ρ ($kg\,m^{-3}$)	992	—
μ_w (Pa s)	658×10^{-6}	—
k_B (J molecule^{-1} K^{-1})	—	1.38×10^{-23} (sucrose)[a]
r_B (m)	—	4.9×10^{-10} (sucrose)[a]
T_{OD} (°K)	303.16	—
ρ_{food} ($kg\,m^{-3}$)	1,040[b]	—
x_I (m)	0.015	—

[a]From Floury et al.[28].
[b]From Fumagalli and Silveira.[24]

TABLE 2
Transport, thermal, and electromagnetic properties of pears

Property	Fresh pear	Osmodehydrated pear
C_{wini}/C_{sini} (°Brix)	0.844/12.8	0.83/14 (20°Brix)
		0.80/18 (40°Brix)
		0.77/21 (60°Brix)
ρ ($kg\,m^{-3}$)	1,000[a]	1,056.7 (20°Brix)[a]
		1,065.5 (40°Brix)[a]
		1,065.5 (60°Brix)[a]
k ($W\,m^{-1}{}^{\circ}C^{-1}$)	0.595[b]	0.514 (20°Brix)[a]
		0.506 (40°Brix)[a]
		0.50 (60°Brix)[a]
C_p ($J\,kg^{-1}\,{}^{\circ}C^{-1}$)	3,600[c]	3,125[d]
ε	$71.06–0.052\ T - 3 \times 10^{-4}\ T^{2e}$	67.3[f]
ε''	$20.95–0.25\ T + 1.4 \times 10^{-3}\ T^{2e}$	13.28 (20°Brix)[f]
		30 (40°Brix)[f]
		23 (60°Brix)[f]

[a]From Agnelli et al.[27]
[b]From Sweat.[35]
[c]From Polley et al.[36]
[d]From Tocci and Mascheroni.[37]
[e]From Sipahioglu and Barringer.[4]
[f]Values in the corresponding range of fruit and sugar solutions.[38]

authors.[13,27] ODmodel-2, which is a simpler model, allowed obtaining moisture values similar to those obtained by ODmodel-1. Using ODmodel-2 in the OD step and the proposed model for MWD, we were able to create a more consistent formulation with a similar level of complexity for description of the combined process but with much less mathematical involvement.

With respect to linking both dehydration processes, the countercurrent flow diffusional model (ODmodel-2) was used to predict initial conditions for microwave drying (Figs. 6a and 6b).

In the first 3 min of the MWD process (Fig. 6b), the weight loss increased as a result of an increase in concentration of the sucrose solution during the OD stage. A higher dehydration rate was reached during microwave drying when the fruits were pretreated with 40 and 60°Brix sucrose solutions. This behavior can be attributed to the change in the dielectric properties promoted by the sugar incorporated during osmotic dehydration. Other authors observed the same phenomenon during microwave freeze drying (MWFD) of potato chips.[34] They studied the drying kinetics during MWFD of raw samples and OD with sucrose solution. They observed that an increase in sugar concentration improved the drying rate, but further increasing sugar concentration from 40 to 50% did not further increase drying rate. This could be attributed to the high uptake of sucrose at high sucrose concentrations that inhibits moisture loss during the microwave drying stage. A reduction of the tissue porosity due to excessive sugar infiltration or possible formation of a peripheral layer of sugar could occur. Previous experiments performed in our laboratory verified the latter assumption. We measured the sugar content profiles in the samples submitted at different sugar solution concentrations and observed a higher sugar content near the sample surface. This could explain the overlap of the predicted curves (40 and 60°Brix) shown in Fig. 6b.

With regard to the evolution of temperature during microwave drying, two well-defined zones can be observed (Fig. 7). During the first heating stage, the temperature increased rapidly and then a constant equilibrium temperature was reached and the change in temperature became

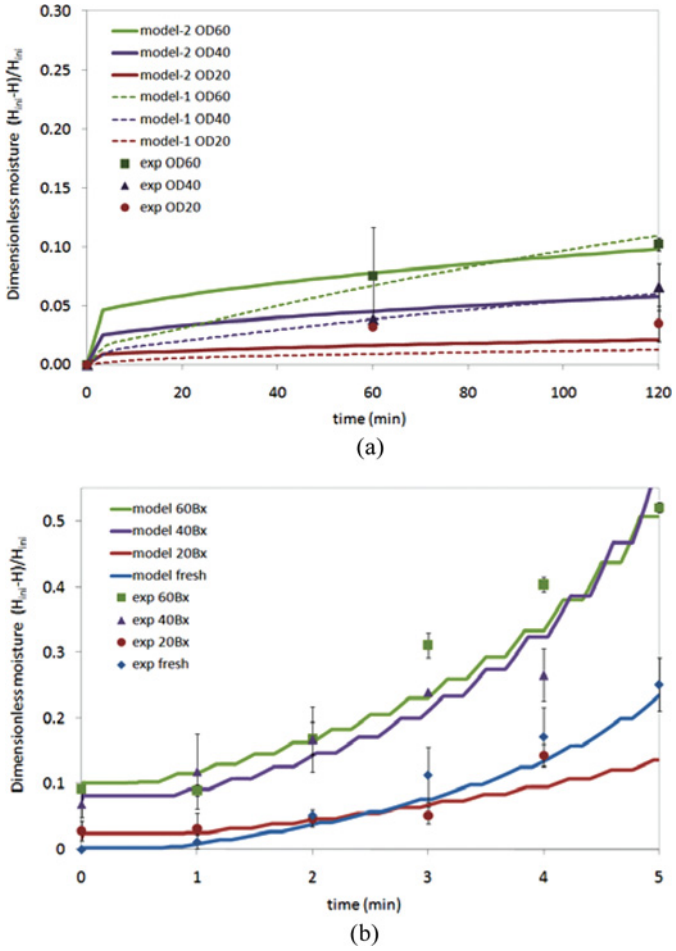

FIG. 6. (a) Experimental (symbols) and predicted values (lines) of moisture loss during osmotic dehydration of pears in sucrose solution of 20, 40, and 60°Brix; (b) Experimental (symbols) and predicted values (lines) of moisture loss during microwave drying of fresh and osmodehydrated pears in sucrose solution of 20, 40, and 60°Brix (color figure available online).

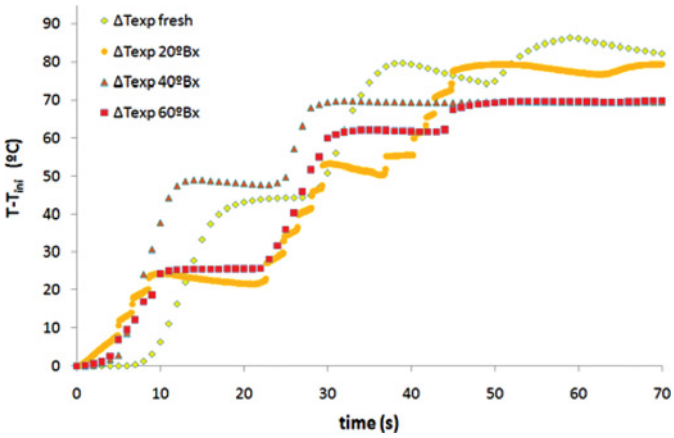

FIG. 7. Experimental increase in temperature ($\Delta T = T - T_{ini}$) during the first 70 s of microwave drying of fresh and osmodehydrated pears (sucrose solutions of 0, 20, 40, and 60°Brix) (color figure available online).

negligible. In the intense heating period (process time less than 50 s), there was no change in temperature during certain time intervals, this behavior occurs for the intermittent cycling operation (on–off). The slope of each experimental curve represents the rate of temperature increase, which is related to the dielectric properties of the fruit.

It can be seen in Fig. 7 that the treatment in 40°Brix sucrose solution promoted the highest rate of temperature change during irradiation, followed by 60°Brix. The lowest slope is presented by pears submitted to 20°Brix solution. Fresh pears show an intermediate temperature increase between the pears pretreated at 40 and 20°Brix. These differences in the slopes can be attributed to the change in dielectric properties due to water loss and solids gain during osmotic pretreatment that affect the capacity of food to transform microwaves into heat. Liao et al.[7] studied the dependence of the dielectric properties of several glucose solutions on concentration. In their analysis, the dielectric properties increased as the solution concentration increased, reaching a maximum at 40°Brix. These results explain the observed behavior of pears with different sugar contents.

With respect to the model's predictive ability (Figs. 8a–8d), the results showed that the numerical model adapted itself correctly to the modifications that occur in the experimental temperature profiles during the intensive heating and equilibrium stages. Additionally, the model properly predicted the on–off control effect of the microwave oven. In this first approach the model did not take into account the overheating stage; therefore, as seen in Figs. 8c and 8d, the model did not follow the increase in temperature after the equilibrium stage in samples pretreated with 40 and 60°Brix sucrose solutions.

Finally, the predictions showed good accuracy for both temperature and moisture content despite the many assumptions made during development of the combined dehydration model.

CONCLUSIONS

A complete and relatively simple and easy-to-use mathematical model was developed for simultaneous prediction of moisture and temperature profiles during the combined process of osmotic–microwave dehydration. Its main contribution is that it can consider the initial process of osmotic dehydration and couple the predicted water and solute concentration profiles to the simultaneous mass and energy transfer in the microwave heating step, including the inner heat generation and the on–off control effect of the microwave oven. In addition, the effect of sugar uptake on microwave drying during the OD process was incorporated into the model formulation.

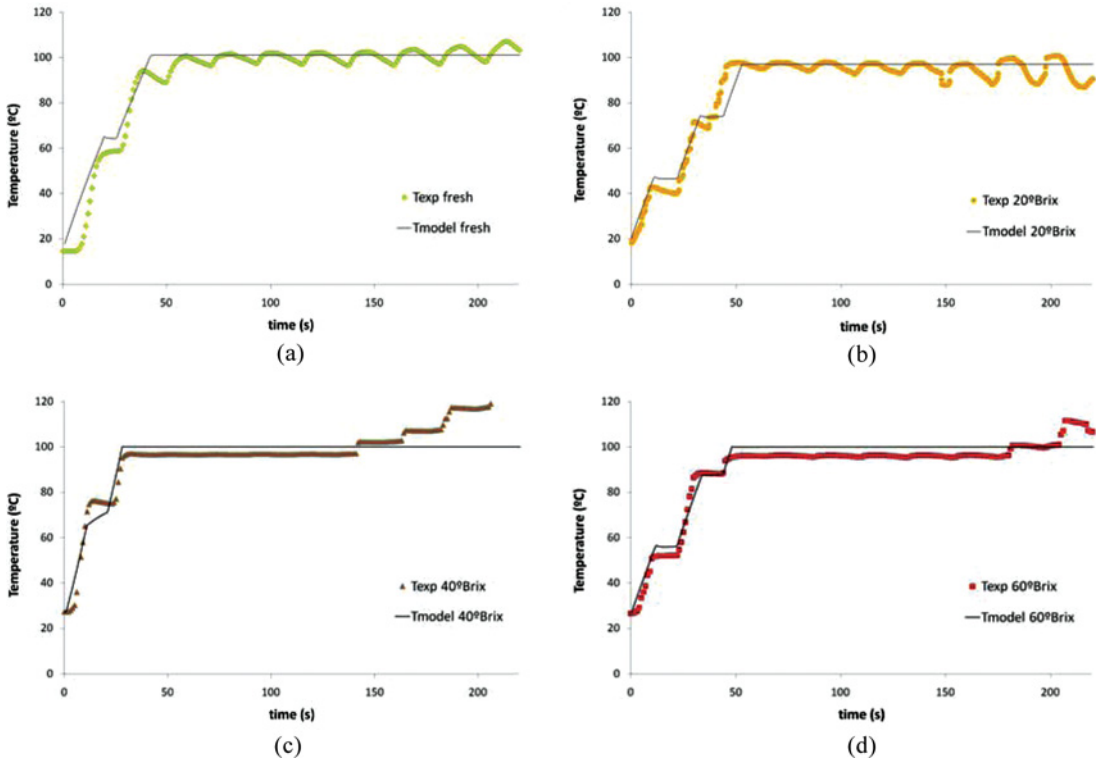

FIG. 8. Experimental and simulated temperature during microwave dehydration of (a) fresh and osmodehydrated pear in sucrose solutions of (b) 20°Brix, (c) 40°Brix, and (d) 60°Brix (color figure available online).

Two models were tested to predict mass transfer during the OD stage. The results had similar accuracy, though the first (ODmodel-1) much more detailed. The main assumptions of ODmodel-2 (as constant volume) do not introduce significant errors due to the short times (up to 120 min) involved in the experimental determinations, which would not involve important weight reduction and its related volume variation.

From the experiments and simulations it can be observed that, in both stages, the weight loss increased as a result of increased concentration of sucrose solution. A higher dehydration rate was reached during microwave drying when the fruits were pretreated with 40 and 60°Brix sucrose solution. This behavior can be attributed to the change in dielectric properties promoted by the sugar incorporated during osmotic dehydration.

Predicted values were in good accordance with experimental determinations. Therefore, the model can be used for the prediction of weight loss in a wide range of operating conditions.

NOMENCLATURE

C	Concentration ($kg\,m^{-3}$)
C_p	Specific heat capacity ($J\,kg^{-1}{}^{\circ}C^{-1}$)
c'_s	Molar concentration of soluble solids ($mol\,m^{-3}$)
D	Diffusion coefficient ($m^2\,s^{-1}$)
$D_{w\text{-}s}$	Binary diffusion coefficient ($m^2\,s^{-1}$)
h	Convective heat transfer coefficient ($W\,m^{-2}{}^{\circ}C^{-1}$)
k	Thermal conductivity ($W\,m^{-1}{}^{\circ}C^{-1}$)
k_B	Boltzmann's constant ($J\,molecule^{-1}\,{}^{\circ}K^{-1}$)
k_m	Mass transfer coefficient ($m\,s^{-1}$)
L	Half-thickness (m)
L_{vap}	Vaporization heat of water ($J\,kg^{-1}$)
m_v	Rate of water vaporization ($kg\,s^{-1}$)
P	Power generated by the absorption of microwaves (W)
P_o	Volumetric absorbed power by the product (W)
P'_o	Power at the surface (W)
Q	Volumetric heat generation ($W\,m^{-3}$)
r_B	Solute apparent hydrodynamic radius (m)
T	Temperature (°C)
T_{OD}	Constant temperature during osmotic dehydration (K)
t	Time (s)
V	Product volume (m^3)
x	Spatial coordinate (m)

Greek Symbols

α	Attenuation factor (m^{-1})
δ	Penetration depth
ε'	Dielectric constant

ε'' Loss factor
λ Wavelength of microwaves (m)
μ_m Viscosity of binary solution (Pa s)
μ_w Water viscosity (Pa s)
ρ Density (kg m^{-3})

Subscripts

a Ambient
d Dehydrated material
eq Equilibrium
ini Initial
OD Osmotic dehydration
s Soluble solids
w Water

ACKNOWLEDGMENT

The authors thank the Faculty of Engineering, La Plata National University, and CONICET and ANPCyT of Argentina for financial support.

REFERENCES

1. Datta, A.K.; Zhang, J. *Porous Media Approach to Heat and Mass Transfer in Solid Foods*; Department of Agriculture and Biology Engineering, Cornell University: Ithaca, NY, 1999.
2. Ryynänen, S. The electromagnetic properties of food materials: A review of basic principles. *Journal of Food Engineering* **1995**, *26*, 409–429.
3. Feng, H.; Tang, J.; Cavalieri, R.P. Dielectric properties of dehydrated apples as affected by moisture and temperature. *Transactions of the ASAE* **2002**, *45*(1), 129–135.
4. Sipahioglu, O.; Barringer, S.A. Dielectric properties of vegetables and fruits as a function of temperature, ash and moisture content. *Journal of Food Science* **2003**, *68*(1), 234–239.
5. Datta, A.K.; Sumnu, G.; Raghavan, G.S.V. Dielectric properties of foods. In *Engineering Properties of Foods*; Rao, M.A., Rizvi, S.S.H., Datta, A.K., Eds.; CRC Press: New York, 2005; 501–565.
6. Liao, X.; Raghavan, V.G.S.; Meda, V.; Yaylayan, V.A. Dielectric properties of supersaturated α-D glucose aqueous solutions at 2450 MHz. *Journal of Microwave Power and Electromagnetic Energy* **2001**, *36*, 131–138.
7. Liao, X.; Raghavan, G.S.V.; Dai, J.; Yaylayan, V.A. Dielectric properties of μ-D-glucose aqueous solutions at 2450 MHz. *Food Research International* **2003**, *36*, 485–490.
8. Azuara, E.; Cortes, R.; Garcia, H.S.; Beristain, C.I. Kinetic model for osmotic dehydration and its relationship with Fick's second law. *International Journal of Food Science and Technology* **1992**, *27*, 239–242.
9. Rahman, M.S.; Sablani, S.S.; Al-Ibrahin, M.A. Osmotic dehydration of potato: Equilibrium kinetics. *Drying Technology* **2001**, *19*(6), 1163–1176.
10. Rastogi, N.K.; Raghavarao, K.S.M.S. Water and solute diffusion coefficients of carrot as a function of temperature and concentration during osmotic dehydration. *Journal of Food Engineering* **1997**, *34*, 429–440.
11. Marcotte, M.; Le Maguer, M. Repartition of water in plant tissue subjected to osmotic processes. *Journal of Food Process Engineering* **1991**, *13*, 297–320.
12. Yao, Z.; Le Maguer, M. Mathematical modelling and simulation of mass transfer in osmotic dehydration processes. Part I: Conceptual and mathematical models. *Journal of Food Engineering* **1996**, *29*, 349–360.
13. Spiazzi, E.A.; Mascheroni, R.H. Mass transfer model for osmotic dehydration of fruits and vegetables. I. Development of the simulation model. *Journal of Food Engineering* **1997**, *34*(4), 387–410.
14. Kaymak-Ertekin, F.; Sultanoğlu, M. Modelling of mass transfer during osmotic dehydration of apples. *Journal of Food Engineering* **2000**, *46*, 243–250.
15. Zhou, L.; Puri, V.M.; Anantheswaran, R.C.; Yeh, G. Finite element modelling of heat and mass transfer in food materials during microwave heating—Model, development and validation. *Journal of Food Engineering* **1995**, *25*, 509–529.
16. Jia, D.; Afzal, M.T. Modeling the heat and mass transfer in microwave drying of white oak. *Drying Technology* **2008**, *26*(9), 1103–1111.
17. Rattanadecho, P.; Aoki, K.; Akahori, M. Experimental and numerical study of microwave drying in unsaturated porous material. *International Communications in Heat and Mass Transfer* **2001**, *28*, 605–616.
18. Sanga, E.C.M.; Mujumdar, A.S.; Raghavan, G.S.V. Simulation of convection–microwave drying for a shrinking material. *Chemical Engineering and Processing* **2002**, *41*, 487–499.
19. Sungsoontorn, S.; Rattanadecho, P.; Pakdee, W. One-dimensional model of heat and mass transports and pressure built up in unsaturated porous materials subjected to microwave energy. *Drying Technology* **2011**, *29*(2), 189–204.
20. Arballo, J.R.; Campañone, L.A.; Mascheroni, R.H. Modelling of microwave drying of fruits. *Drying Technology* **2010**, *28*, 1178–1184.
21. Venkatachalapathy, K.; Raghavan, G.S.V. Combined osmotic and microwave drying of strawberries. *Drying Technology* **1999**, *17*, 837–853.
22. Beaudry, C.; Raghavan, G.S.V.; Rennie, T.J. Microwave finish drying of osmotically dehydrated cranberries. *Drying Technology* **2003**, *21*(9), 1797–1810.
23. Beaudry, C.; Raghavan, G.S.V.; Ratti, C.; Rennie, T.J. Effect of four drying methods on the quality of osmotically dehydrated cranberries. *Drying Technology* **2004**, *22*(3), 521–539.
24. Fumagalli, F.; Silveira, A.M. Quality evaluation of microwave-dried Packham's triumph pear. *Drying Technology* **2005**, *23*, 2215–2226.
25. Andrés, A.; Fito, P.; Heredia, A.; Rosa, E.M. Combined drying technologies for development of high-quality shelf-stable mango products. *Drying Technology* **2007**, *25*(11), 1857–1866.
26. Corrêa, J.L.G.; Dev, S.R.S.; Gariepy, Y.; Raghavan, G.S.V. Drying of pineapple by microwave–vacuum with osmotic pretreatment. *Drying Technology* **2011**, *29*(13), 1556–1561.
27. Agnelli, M.E.; Marani, C.M.; Mascheroni, R.H. Modelling of heat and mass transfer during (osmo) dehydrofreezing of fruits. *Journal of Food Engineering* **2005**, *69*(4), 415–424.
28. Floury, J.; Le Bail, A.; Pham, Q.T. A three-dimensional numerical simulation of the osmotic dehydration of mango and effect of freezing on the mass transfer rates. *Journal of Food Engineering* **2008**, *85*, 1–11.
29. Lin, Y.E.; Anantheswaran, R.C.; Puri, V.M. Finite element analysis of microwave heating of solid foods. *Journal of Food Engineering* **1995**, *25*, 85–112.
30. Pauli, M.; Kayser, T.; Adamiuk, G.; Wiesbeck, W. Modeling of mutual coupling between electromagnetic and thermal fields in microwave heating. In *Proceedings of Microwave Symposium—IEEE/MTT-S International*, Honolulu, HI, June 3–8, 2007; 1983–1986.
31. Bird, R.B.; Stewart, W.E.; Lightfoot, E.N. *Transport Phenomena*; John Wiley & Sons: New York, 1976.

32. Association of Official Analytical Chemists. *Official Methods of Analysis of the Association of Official Analytical Chemists*, 17th Ed; Association of Official Analytical Chemists: Gaithersburg, MD, 2000.
33. Torregiani, D. Osmotic dehydration in fruit and vegetables. *Food Research International* **1993**, *26*, 59–68.
34. Wang, R.; Zhang, M.; Mujumdar, A.S. Effect of osmotic dehydration on microwave freeze-drying characteristics and quality of potato chips. *Drying Technology* **2010**, *28*(6), 798–806.
35. Sweat, V.E. Experimental values of thermal conductivity of selected fruits and vegetables. *Journal of Food Science* **1974**, *39*, 1080–1083.
36. Polley, S.L.; Snyder, O.P.; Kotnour, P. A compilation for thermal properties of foods. *Food Technology* **1980**, *34*, 76–94.
37. Tocci, A.M.; Mascheroni, R.H. Determination by differential scanning calorimetry of the heat capacity and enthalpy of partially dehydrated fruit in concentrated aqueous solutions of sugar. In *Proceedings of I Congreso Ibero-Americano de Ingeniería de Alimentos*, Vol. 1; Campinas, Sao Paulo, Brazil, November 5–9, 1995; 411–420 (in Spanish).
38. Datta, A.K.; Anantheswaran, R.C. *Handbook of Microwave Technology for Food Applications*; Marcel Dekker: New York, 2001.